

Raman spectroscopy of crude oils and hydrocarbon fluid inclusions: A feasibility study

DANIEL ORANGE,* ELISE KNITTLE, DANIEL FARBER,† and QUENTIN WILLIAMS

Department of Earth Sciences and Institute of Tectonics, University of California, Santa Cruz, CA 95064, U.S.A.

Abstract—Visible Raman spectroscopy provides useful constraints on the structure and maturity of both hydrocarbon fluid inclusions and crude oils. In particular, the presence or absence of hydrocarbon functional groups may be qualitatively identified, as well as relative degrees of maturation. The primary constraints on the utility of this technique are: 1) spectral contamination by fluorescence of either the hydrocarbon inclusion or the matrix in which it sits; and 2) photodegradation of hydrocarbons under laser excitation. Both of these difficulties can be averted through a combination of appropriate selection of the laser excitation line and minimization of the excitation volume of fluorescence. We present and interpret spectra of synthetic hydrocarbon inclusions, natural hydrocarbon inclusions contained in a matrix fluorescent under blue-green laser excitation ($\text{CaCO}_3\text{:Mn}$) from the Hoh Accretionary Complex (Olympic Peninsula, Washington), and of crude oils collected from the same region. The latter two types of samples demonstrate the utility of this technique in providing constraints on the structural differences between natural hydrocarbons.

INTRODUCTION

ORGANIC MATTER is present in all sedimentary material, and when such sediment undergoes diagenesis, catagenesis, and metamorphism, this material can be transformed into organic liquids and gases (TISSOT and WELTE, 1984; GAUTIER *et al.*, 1985). Organic fluids present in rock include hydrocarbons ranging from methane to high molecular weight hydrocarbons (KVENVOLDEN and ROEDDER, 1971), and these fluids can undergo complex chemical changes depending on the conditions present during their migration and maturation. Hydrocarbon inclusions are direct samples of the fluid present at that time, and can provide information on the composition of as well as the conditions under which the fluids were emplaced (ROEDDER, 1984). Hydrocarbon inclusions are thus of interest because their compositions are sensitive to the complex interplay between source, transport, and deposition, while the variation in composition between present-day crude oils and inclusions can provide information on the genesis of the fluid (*e.g.*, JENSENIUS and BURRUSS, 1990; MCLIMANS, 1987; ROEDDER, 1984; BURRUSS *et al.*, 1985; NOONER *et al.*, 1973; PERING, 1973). Numerous studies, principally optical, fluorescence, and gas chromatographic measurements, have been conducted on hydrocarbon inclusions to elucidate the evolution of

organic material under a range of geological conditions (PIRONON and BARRES, 1990; JENSENIUS and BURRUSS, 1990; ETMINAN and HOFFMAN, 1989; MCLIMANS and VIDETICH, 1987; MCLIMANS, 1987; PAGEL *et al.*, 1986; HORSFIELD and MCLIMANS, 1984; BURRUSS *et al.*, 1985; KVENVOLDEN and ROEDDER, 1971; MURRAY, 1957).

Distinct advantages exist for techniques able to probe individual hydrocarbon fluid inclusions: their composition (and all the information contained therein) may be placed in a relative temporal sequence based on cross-cutting relationships with microfabrics and with inclusions in other veins and cements (MCLIMANS, 1987). Temporal variations in the chemical composition of hydrocarbons within a region can thus provide information on the evolution of these fluids (TISSOT and WELTE, 1984). By analyzing inclusions on a grain by grain basis, it may be possible to differentiate inclusions from radically different reservoirs, as well as inclusions formed by mixing of different sources. When placed in a diagenetic/structural/temporal framework, the compositions of crude oils and hydrocarbon inclusions potentially allow constraints to be placed on the timing of fluid transport events, the reservoirs involved in each event, and on the maximum temperatures attained by the material present in the inclusion (MCLIMANS, 1987; ROEDDER, 1984; TISSOT and WELTE, 1984).

Typically, compositional studies of individual inclusions have been conducted using vibrational spectroscopic techniques. Analyses of hydrocarbon inclusions have been conducted using infrared spectroscopic techniques (PASTERIS *et al.* 1983;

Present address: *Monterey Bay Aquarium Research Institute, P.O. Box 628, Moss Landing, CA 95039, U.S.A. and †Dept. of Earth and Space Sciences, University of California, Los Angeles, CA 90024, U.S.A.

BARRES *et al.*, 1987; GUILHAUMOU and SZYDLOWSKI, 1989; O'GRADY *et al.*, 1989; WOPENKA *et al.*, 1990; PIRONON and BARRES, 1990), yet such measurements are limited by diffraction effects to inclusions larger than $\sim 15 \mu\text{m}$ in diameter (WOPENKA *et al.*, 1990), and a number of hydrocarbon vibrations are weak or inactive in the infrared (DOLLISH *et al.*, 1974). Raman spectroscopic techniques, although frequently applied to inorganic inclusions, have been underutilized in the study of hydrocarbon inclusions. Indeed, studies on natural organic inclusions have been primarily conducted on methane-bearing assemblages, particularly those in the $\text{N}_2\text{-CO}_2\text{-CH}_4$ system (CHOU *et al.*, 1990; PASTERIS *et al.*, 1985, 1988; SEITZ *et al.*, 1987, 1989). Exceptions to this include the study of DELE-DUBOIS *et al.* (1980) on hydrocarbon (possibly pentane) inclusions in emerald, and that of GUILHAUMOU *et al.* (1988) who, although unable to spectroscopically characterize fluorescent primary and secondary inclusions, were able to analyze for methane, ethane, and propane in vapor-dominated inclusions. PIRONON and BARRES (1990) obtained spectra of a single hydrocarbon inclusion with exceptionally low fluorescence, and interpreted their results as indicating the presence of n-heptane and a minor amount of aromatics.

Raman spectra of more complicated hydrocarbon inclusions are considerably less common: this originates in the perception that these studies are difficult or impossible (ROEDDER, 1984; TOURAY *et al.*, 1985; BURRUSS *et al.*, 1989). The usual reasons cited for the lack of feasibility of such measurements are several: first, the presence of laser-induced fluorescence from both natural hydrocarbons and many host minerals can overwhelm the Raman scattering signal (ROSASCO and ROEDDER, 1979; GUILHAUMOU, 1982; TOURAY *et al.*, 1985; GUILHAUMOU *et al.*, 1988; WOPENKA *et al.*, 1990); second, laser-induced photodegradation may alter the chemical composition of the inclusion (TOURAY *et al.*, 1985; GUILHAUMOU, 1982); and finally, the low laser power per area required in studies of these inclusions would make the Raman scattering intensity correspondingly low (TOURAY *et al.*, 1985; ROSASCO and ROEDDER, 1979).

Although each of these criticisms has merit for Raman experiments on natural inclusions using either blue or green laser lines of the argon-ion lasers used in many Raman laboratories, one of the intents of this paper is to demonstrate that a judicious choice of laser excitation, coupled with photon counting detection and a low incident laser intensity, render Raman spectra of highly fluorescent

natural inclusions in a fluorescent matrix feasible, if not routine. In particular, the utilization of a laser which is not absorbed by either the inclusion or the host mineral is critical for the success of such measurements.

Recently, PIRONON *et al.* (1991) have reported Raman spectra in the C—H stretching region of several hydrocarbon inclusions using Fourier Transform-Raman spectroscopy with excitation at 1064 nm. In this study we will first demonstrate that the interferometer and specialized infrared laser and optical system necessary for FT-Raman measurements is not mandatory for conducting Raman spectroscopy on complex hydrocarbon fluid inclusions (indeed, they may be conducted with equipment available in many Raman labs). Secondly, we will demonstrate the ability of this non-destructive technique to identify different functional units within (and thus, on the thermal and geochemical history of) hydrocarbon inclusions.

In addition to providing information on the chemistry of the inclusions, Raman spectroscopy also has the advantage of having extremely small spatial resolution (as small as $2 \mu\text{m}$; PASTERIS *et al.*, 1988). Thus, it is possible to carry out studies on an inclusion by inclusion basis in a sample, thereby characterizing multiple phases of fluid interaction. These individual inclusions can also be compared with present-day crude oils to examine differences in hydrocarbon composition, information that may relate to the evolutionary history of both the host rock and the oil.

In this paper, we present a study of a suite of synthetic hydrocarbon fluid inclusions, n-pentadecane, bromobenzene and cyclohexane, to illustrate the feasibility of studying fluorescent hydrocarbons using Raman spectroscopy. We then apply the technique to two fluorescent and chemically complex crude oils from the Hoh accretionary complex, Olympic Peninsula, Washington. Previous gas chromatographic studies of these oils indicate that they are similar in composition: our results are in accord with these analyses (KVENVOLDEN *et al.*, 1989). Finally, we present an analysis of a representative natural hydrocarbon fluid inclusion. This inclusion occurs in rocks located near the crude oils, although the inclusions were trapped in the Miocene (ORANGE *et al.*, 1993). The inclusion is qualitatively similar in structure to the crude oils, yet differs in several important respects that may reflect a different migration history.

EXPERIMENTAL METHODS

Raman system

The Raman spectra of the synthetic fluid inclusions were collected using a Coherent Innova 70-4 argon-ion

laser tuned at 488 nm. An Optometrics laser monochromator was used to remove plasma lines, and the laser beam at the sample was attenuated to between 1 and 5 mW. A modified Leitz Orthoplan microscope is used to image the fluid inclusions and to focus the laser into the sample. The microscope is fitted with a Leitz UM 32X objective to focus the laser and collect the scattered light in a 0 degree backscattering geometry. An aperture in the microscope system is used to isolate the sample area containing the fluid inclusion. The scattered light is then focused with an Olympus camera lens into the front slit of a SPEX Triplemate spectrograph equipped with a 600 gr/mm holographic grating in the filter stage and a 1200 gr/mm holographic grating in the spectrograph stage. Spectra are collected using a thermoelectrically cooled ITT Model F4146 two-dimensional micro-channel plate controlled by a Surface Sciences Laboratory Position Computer (Quantar Technologies). This detector couples the photon-counting resolution, high quantum efficiency and high signal to noise of a conventional photomultiplier tube with the two dimensionality of CCD detectors (VEIRS *et al.*, 1987). Because of the photon-counting ability of this detector and the ability to collect spatially resolved data in a spectrographic mode (that is, without scanning a monochromator), we are able to collect Raman data using extremely low incident light levels. Typical exposure times for these inclusions were 1 to 6 hours.

For the natural fluid inclusion and the crude oils studied, a Uniphase 18 mW He—Ne laser (632.8 nm) was used for sample excitation: both the natural fluid inclusions and the crude oils, as well as the host calcite matrix of the natural inclusions, strongly fluoresce at argon-ion wavelengths (488.0 and 514.5 nm), so a red laser was used to minimize sample absorbance and fluorescence. Oil samples were contained in fused silica microtubes. Laser plasma lines were removed with a standard Oriol laser-line filter, and the laser power at the sample was again between 1 and 5 mW. For the natural fluid inclusions, a Leitz 100X microscope objective was used to focus the laser beam into the inclusion and collect the scattered light. The exposure times for the Raman scattering were 12 to 24 hours. The low levels of Raman excitation used did not cause detectable photodegradation in either the oils or fluid inclusions, as manifested by either a change in visual appearance of the inclusion, or by any time dependence of the spectra.

Sample preparation

J. Pironon of CREGU (France) provided synthetic n-pentadecane, bromobenzene and cyclohexane fluid inclusions. These inclusions are made using a technique described elsewhere (PIRONON, 1990), and are typically 10–50 μm in diameter. In contrast to most natural inclusions, these synthetic inclusions were contained in high purity KCl, which not only does not fluoresce, but also has no first-order Raman spectrum. Moreover, these samples are thick and monocrystalline, reducing the amount of stray scattered light from the sample. Thus, the solid matrix containing the synthetic inclusions is comparatively ideal for Raman spectroscopic measurements. We limited the light intensity incident on the sample to less than 5 mW in all cases, and utilized highly attenuated Ar-ion laser light to obtain spectra of these inclusions (~ 1 mW).

Natural hydrocarbon fluid inclusions were obtained from a suite of rocks collected from the Hoh rock assem-

blage of the western Olympic peninsula, Washington (RAU, 1973, 1975, 1979). The natural hydrocarbon fluid inclusions occur most frequently in syn-deformational sparitic calcite veins. These inclusions range from 2 to 60 μm in long dimension, and are commonly in the 5 to 15 μm range. Inclusions vary in color from translucent to light brown to dark brown, and fluoresce strongly (under incident UV) in colors ranging from blue to greenish yellow (~ 485 – 535 nm). Highly polished standard thin sections (30 mm thick) were prepared from the Hoh rock samples for petrographic and Raman analysis. These were separated from their supporting glass slides, and the rock chip was mounted on a block of NaCl, as halite has no first order Raman spectrum. The use of kerosene was avoided in all parts of the sample preparation process because of possible interference of hydrocarbon contamination with the Raman analyses of the fluid inclusions. Extensive polish helped prevent excess light scattering off surface topography of the sample.

We initially examined thin sections of samples using optical and cathodoluminescence petrography in order to clarify the relative cross-cutting relationships between the fluid inclusions and the microstructures of the sample (ORANGE *et al.*, 1993). We then carried out detailed optical and ultraviolet fluorescence petrography to identify potential hydrocarbon inclusions. Inclusions that appeared light tan to dark brown in visible light and fluoresced under ultraviolet light were selected for further study using Raman spectroscopy. Both the manganese-bearing calcite matrix and the complex hydrocarbons present within these inclusions necessitated utilization of He—Ne laser excitation to produce Raman spectra.

BACKGROUND

The three primary experimental difficulties in Raman spectroscopy of fluid inclusions are: 1) laser-induced fluorescence from the solid matrix holding the inclusion; 2) fluorescence from the material of the inclusion itself; and 3) laser-induced photodegradation within the inclusion. The first of these problems is endemic to all inclusions within certain types of minerals: the example of primary relevance to this study is that of calcite with Mn^{2+} as a trace substituent. The latter two problems, inclusion fluorescence and photodegradation, are each primarily associated with hydrocarbon inclusions, and are generated by the range of energies of anti-bonding excited electronic states available to complex hydrocarbons. In the following discussion, we emphasize the fluorescence behavior of hydrocarbons present in moderately mature inclusions (falling generally toward the blue end of the visible spectrum under UV excitation). In particular, we focus on the fluorescence and photodegradation (or lack thereof) undergone by alkanes (paraffins), cycloalkanes (naphthenes), and aromatics (particularly benzenoids) under various types of laser irradiation. We explicitly do not treat more complex organic compounds of limited abundances

and thermal stabilities, such as porphyrin-based materials. Our intent is to document that for a range of hydrocarbon inclusions, both laser-induced sample photodegradation and sample fluorescence can be reduced to noninterfering levels, and that significant qualitative insight into the molecular species present within these inclusions (and thus insight into their thermal and chemical histories) may be gained from appropriately collected Raman spectra.

Notably, both photodegradation and fluorescence are critically dependent upon the absorption spectrum of the inclusion or host mineral: as a result, these problems may be avoided by an appropriate choice of the Raman excitation wavelength. That is, avoiding the absorption bands of a hydrocarbon is crucial when choosing a Raman excitation line. We utilize this relatively straightforward approach to determine spectra of both our natural and synthetic inclusion samples. Our guiding principle is to use the highest frequency (lowest wavelength) laser line feasible for each mineral/inclusion pair: this choice is motivated by the (generally) higher detector sensitivity for higher frequency photons and by the enhanced Raman scattering efficiency obtainable at shorter excitation wavelengths.

Solid matrix fluorescence

In this discussion, we deal principally with the example of Mn^{2+} impurity fluorescence within the calcite lattice. Although the fluorescent characteristics of each host mineral (or its associated impurities) with inclusions of interest should be evaluated on an individual basis prior to Raman spectral study, we consider the case of $CaCO_3:Mn^{2+}$ to represent a particularly severe test for visible laser-induced Raman scattering measurements. The difficulties associated with this mineral (and specifically our samples of this mineral) are several-fold. First, the fluorescence of manganese in these samples of calcite is intense and, under blue excitation, overwhelms the Raman signal from not only the inclusion, but also the host calcite. This fluorescence intensity is particularly large in calcite partially because the quenching ability of other ions, particularly Fe^{2+} , in calcite is low (MEDLIN, 1968; TEN HAVE and HEIJNEN, 1985). Second, the $Mn^{2+} T_{1g} \rightarrow A_{1g}$ emission band lies between 520 and 730 nm, a region of primary interest for Raman scattering experiments using blue laser excitation (MEDLIN, 1968; WALKER *et al.*, 1989). Finally, the absorption bands which pump the emission band

of manganese in calcite span much of the visible region of the spectrum from 450 to 630 nm (MEDLIN, 1968; WALKER *et al.*, 1989).

Despite its fluorescent characteristics, we note the importance of being able to conduct Raman spectral measurements on hydrocarbon fluid inclusions in a calcite matrix containing transition-metal ion impurities. Because liquid hydrocarbons form in a comparatively low pressure, low temperature environment, inclusions containing such fluids are frequently found in calcite veins.

In order to measure Raman spectra in this matrix, we utilized the 632.8 nm line of a He-Ne laser to produce Raman spectra of the natural inclusions, instead of the more commonly used Ar-ion emission lines at 457.9, 488.0 and 514.5 nm. The 632.8 nm line of He-Ne, although significantly less powerful (for lasers of comparable expense) than those of the argon-ion laser, has the advantage that the resultant fluorescence of calcite is extremely low, and thus the line is able to produce Raman spectra of acceptable quality. The physical mechanism behind this improvement is simple: the incident laser wavelength is chosen so that the sample absorption (and thus emission) is minimized. A spectra produced under these conditions of a non-inclusion bearing monocrystalline region of this calcite from the Hoh accretionary prism is shown in Fig. 1. No significant fluorescence is observed, and the primary Raman lines of the calcite spectrum are well-resolved, as is the isotopically shifted component of the strong symmetric stretching vibration of the carbonate unit (inset, Fig. 1). Because this spectrum is of a non-oriented single crystal, the relative peak intensities differ somewhat from those of calcite powder, although their location is in excellent agreement with previous studies (*e.g.*, WHITE, 1974). Notably, either a Kr-ion laser or red-tuned dye laser could be used with similar effect (and with potentially greater power). Thus, judicious selection of an appropriate visible (or infrared) laser line can minimize or eliminate the effects of unwanted mineral fluorescence in Raman spectra of fluid inclusions in calcite. We note that the alternative technique of time lapse spectroscopy, which takes advantage of the long lifetime of fluorescence relative to vibrational measurements, can also be utilized to eliminate fluorescence effects (*e.g.*, FRANTZ *et al.*, 1982).

Petroleum fluorescence and laser-induced photodegradation

The relatively high absorption of many hydrocarbon inclusions in the ultraviolet and resultant

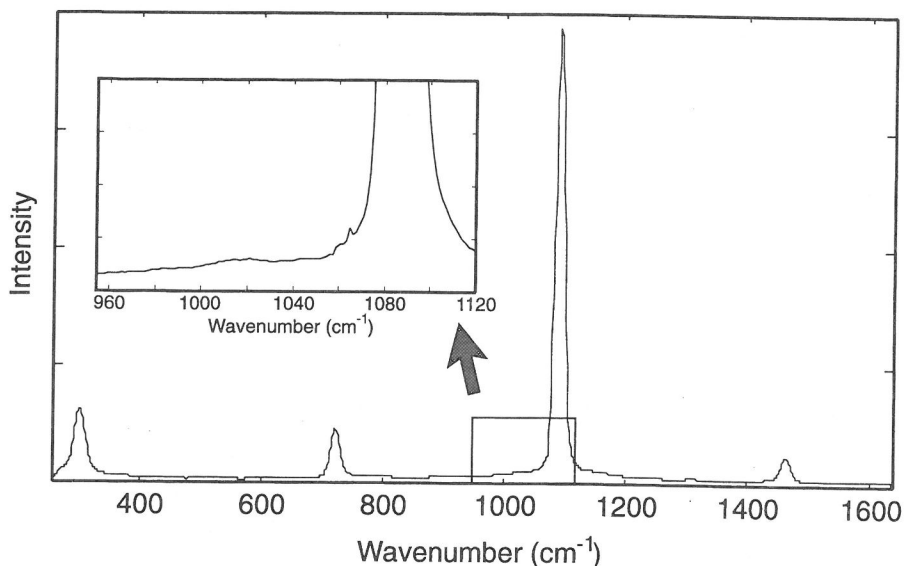


FIG. 1. Raman spectrum of manganese-bearing calcite from the Hoh accretionary peninsula: the spectrum was produced using 632.8 nm excitation to avoid manganese-induced sample fluorescence. The inset shows the spectral feature associated with the symmetric stretching vibration of carbon-13 bearing carbonate groups.

visible fluorescence (note that for simplicity we do not distinguish between fluorescence and phosphorescence of hydrocarbons, but use the former term to describe all light emission associated with relaxation of electronic excited states) has been widely used to verify the presence of hydrocarbons within fluid inclusions (BURRUSS, 1981; BURRUSS *et al.*, 1983, 1985; HASZELDINE *et al.*, 1984; HORSFIELD and MCLIMANS, 1984; PAGEL *et al.*, 1986; GUILHAUMOU *et al.*, 1988; JENSENIUS and BURRUSS, 1990). Because of the high flux of photons associated with laser Raman measurements, as well as the relative weakness of the spontaneous Raman effect (efficiencies typically of order 10^{-6} ; NAKAMOTO (1982)), even a small amount of sample absorption (and reemission) may induce a sufficient amount of fluorescence to interfere with the Raman spectrum. The most efficient mechanisms by which hydrocarbons fluoresce is by transitions from bonding or non-bonding states to anti-bonding states, principally either $\pi \rightarrow \pi^*$ or $n \rightarrow \pi^*$ transitions, followed by subsequent radiative relaxation to the ground state (*e.g.*, BECKER, 1969). The lower energy of the resultant fluorescent photon from that of the initial excitation photon is primarily produced by the environment of the excited molecule shifting to a lower energy configuration following the excitation, but prior to emission. This phenom-

enon is described by the Franck-Condon effect (*e.g.*, ENGLMAN, 1979).

Notably, in contrast to the Raman effect, characteristic quantum efficiencies of the fluorescence of organic compounds (particularly aromatics) are high: typically between 0.05 and 0.99 (DAWSON and WINDSOR, 1968). It is these high efficiencies, when coupled with the comparative weakness of the Raman effect, which have rendered characterization of the Raman spectra of hydrocarbon fluid inclusions difficult: even a trace quantity of hydrocarbons which fluoresce under the incident laser excitation can generate a background larger than that of the Raman scattering from the sample.

Fortunately, the primary absorption bands of simple alkanes and cycloalkanes fall below 200 nm in wavelength. The major simple ($C_n < \sim 30$) naturally-occurring carbon compounds with absorption bands which can either be present in, or tail into, the blue region of the visible are either aromatic compounds (particularly those with multiple rings) or polyolefins with $C_n > \sim 10$. For most hydrocarbons of this type, absorption seldom extends to wavelengths higher than about 550 nm (BERLMAN, 1965; DIAS, 1987; BURDETT and TAYLOR, 1955). We note in this context that extremely immature hydrocarbons with significantly more complex molecules might require infrared excitation to avoid sample absorption/fluorescence (*e.g.*, PIR-

ONON *et al.*, 1991). However, for inclusions varying in net complexity from methane, ethane, and other alkanes (*e.g.*, SEITZ *et al.*, 1987; GUILHAUMOU *et al.*, 1988; PIRONON and BARRES, 1990) to those with hydrocarbons of intermediate complexity, most complex hydrocarbon fluorescence and/or photodegradation can again be avoided by utilization of an appropriate visible (in this case, red) laser line.

In this context, it is of critical importance to examine any hydrocarbon inclusions for visible absorption prior to Raman spectral characterization. In the case of each of the synthetic hydrocarbons we have examined, the absorption spectra of the hydrocarbons are well-known (*e.g.*, BERLMAN, 1965; *Sadtler Handbook of UV Spectra*, 1982), and each is amenable to examination using either the 488.0 or 514.5 nm lines of argon-ion lasers. This is again in contrast to the case of the natural inclusions examined, which not only fluoresce under excitation at these frequencies, but also appear to undergo photodegradation. The 632.8 nm line of the He-Ne laser avoids not only the problem of fluorescence but also, by implication, that of photodegradation.

Photodegradation of hydrocarbons results from the enhanced reactivities of molecules within their excited states: in this sense, photodegradation and fluorescence represent competitive processes of non-radiative and radiative decay of excited states (*e.g.*, COWAN and DRISKO, 1976). Although small amounts of photodegradation are difficult to preclude from having occurred within our natural inclusions, we are confident that photodegradation from 632.8 nm excitation does not result in any major changes in the chemical species present within these inclusions. Our rationales for this are several-fold. First, no time-dependence of the spectra is observed (other than the normal increase in signal to noise for longer collection times). Neither are there any observable changes in the physical appearance of the inclusion during or following laser-irradiation (for reference, under argon-ion excitation, these inclusions were observed to darken in color and seep into cleavage planes in the calcite, indicating that the material in the inclusion had undergone both a chemical change and a decrease in viscosity). Finally, the lack of fluorescence from these samples, as well as their apparent transparency to red light, implies that any absorption in the sample at this wavelength must be weak.

RESULTS AND DISCUSSION

Synthetic fluid inclusions

n-Pentadecane. The *n*-pentadecane ($C_{15}H_{32}$) inclusion studied is a colorless, pseudospherical, one-

phase inclusion, 35 mm in diameter. Under long-wavelength ultraviolet light (366 nm Hg) the *n*-pentadecane inclusion exhibits medium intensity impurity fluorescence in a dull green color (~ 530 nm). This fluorescence was manifested as a broad, low amplitude signal centered at 1800 cm^{-1} away from the incident 488 nm laser line, with a half-wavelength of $\sim 300\text{ cm}^{-1}$. We note that the impurity level in these samples is likely to be one part in 10^3 - 10^6 . The fluorescence peak was small and centered away from any peaks of interest, and thus presented no difficulties in terms of collecting Raman spectra. The spectra for this inclusion with peak assignments (*e.g.*, DOLLISH *et al.*, 1974) are shown in Fig. 2a.

PIRONON and BARRES (1990) published infrared and Raman spectra of these pentadecane inclusions in the C—H stretching spectral region (between 2850 and 2975 cm^{-1}) using both synthetic inclusions and a liquid standard. Their peak identifications for both the standard and the inclusion are identical to those of this study; our spectra (Fig. 2) however, show a stronger methyl C—H symmetric stretch (2848 cm^{-1}), and resolve a number of side peaks (possibly combination bands). PIRONON and BARRES (1990) also identify a small peak at 2730 cm^{-1} which we do not observe in our spectra. Many of the bands of these synthetic hydrocarbons (such as the C—H stretching vibrations) are endemic to hydrocarbons, and are accordingly not particularly useful in determining the presence or absence of different structural groups. Instead, we focus on bands which allow us to discriminate between functional groups, in order to produce particular regions of interest for unknown inclusions. For example, the vibrations centered at 1440 cm^{-1} are due to the methylene scissors vibration, and therefore are dependent on the presence of $-\text{CH}_2-$ groups; peaks near this vibrational frequency are indicative of alkanes and cycloalkanes.

Cyclohexane. The cyclohexane (C_6H_{12}) occurs as numerous pseudospherical inclusions ranging from 25 to 80 mm in diameter. The vast majority of these inclusions are one phase, although several contain a small bubble (probably aqueous) as well. Under long wavelength ultraviolet light (366 nm Hg) these inclusions exhibit an extremely subtle impurity fluorescence in a very dark red color (~ 635 nm). Using the Argon-ion 488 nm laser line for the Raman spectra, this fluorescence will appear at a wave number shift much higher than the C—H stretching vibration; we thus expect no interference from this fluorescence with the Raman spectra. The spectra and peak assignments are shown in Fig. 2b.

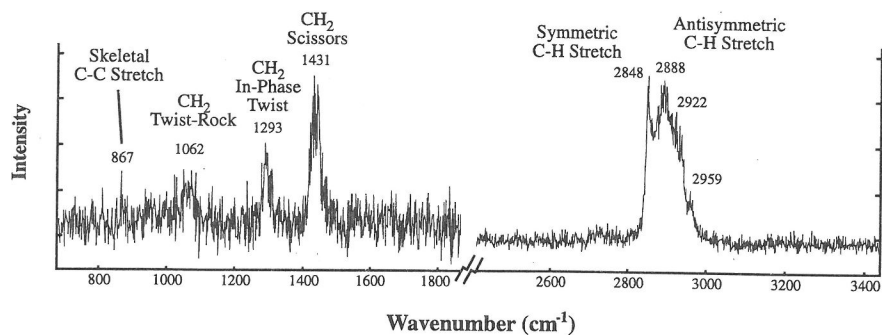
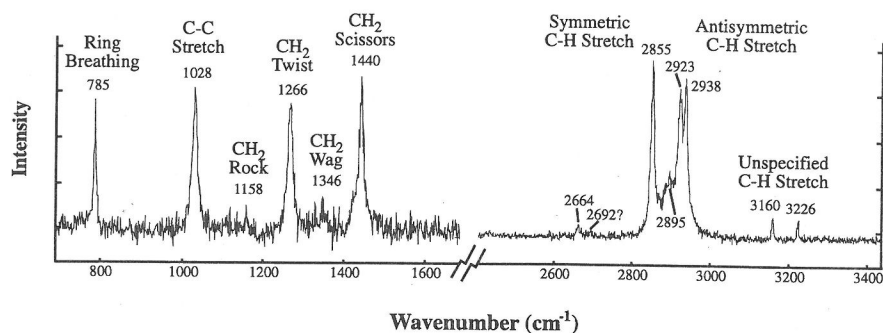
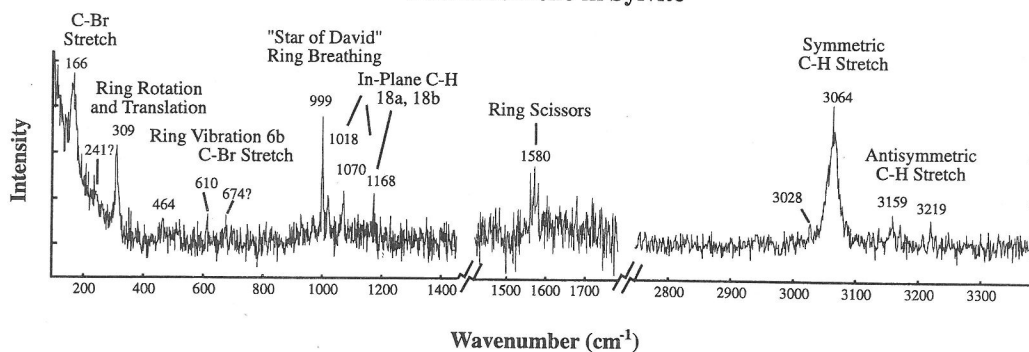
n-Pentadecane in Sylvite**Cyclohexane in Sylvite****Bromobenzene in Sylvite**

FIG. 2. Raman spectrum of synthetic a) n-pentadecane, b) cyclohexane, and c) bromobenzene inclusions in sylvite. Note that the collection times, and thus the intensity scales, are different for each spectral region.

Our Raman spectrum of the cyclohexane inclusion matches in both peak location and relative intensity the cyclohexane Raman bands found in PRONON's (1990) spectra of a cyclohexane standard or a syn-

thetic inclusion containing 50% cyclohexane and 50% bromobenzene. The spectra shown in Fig. 2b, however, better resolve the details of the manifold (in particular, the 2895 cm⁻¹ methyl symmetric

C—H stretch) due to the high signal to noise of our system. Note also that the small C—H stretch peak at 2664 cm^{-1} is resolved, illustrating the sensitivity of this system.

The strong peaks at 785 cm^{-1} and 1028 cm^{-1} (Fig. 2b) are diagnostic of cyclohexane and represent the vibrations for ring-breathing and C—C stretching vibrations, respectively. Although the position of the ring breathing peak can change slightly as a function of substituted groups, strong peaks in the 700 cm^{-1} to 1000 cm^{-1} range can signify the presence of cycloalkanes.

Bromobenzene. Bromobenzene ($\text{C}_6\text{H}_5\text{Br}$) inclusions occur as pseudospherical, one phase (and rare two-phase) inclusions ranging in diameter from 15 to 30 mm. Under long wavelength ultraviolet light (366 nm Hg) the impurities in the bromobenzene inclusions fluoresce slightly in a light blue color ($\sim 505\text{ nm}$). The inclusion fluorescence in this sample was again low and centered away from peaks of interest; we were therefore able to collect quality spectra using the Argon ion 488 nm laser line. The Raman spectra with identified peaks (DOLLISH *et al.*, 1974) are illustrated in Fig. 2c. Our Raman spectrum of the bromobenzene inclusion matches in both peak location and intensity, over the regions of overlap (i.e. the mid- and hi-frequency regions), the bromobenzene Raman bands found in PIRONON'S (1990) published spectra of a bromobenzene standard and a synthetic inclusion with 50% cyclohexane and 50% benzene.

The very strong peak at 999 cm^{-1} is due to the breathing vibration of the benzene ring; within end-member benzene, this band has A_{1g} symmetry, and involves simultaneous inward and outward motion of all the carbon atoms (DOLLISH *et al.*, 1974; LINVIEN *et al.*, 1991). Within substituted benzenes, the trigonal "Star of David" vibration, derived from the infrared-active B_{1u} symmetry mode of end-member benzene, is Raman active. This mode involves alternate inward and outward motions of the carbon atoms within the plane of the ring, and lies at nearly the same energy as the A_{1g} breathing vibration. In some cases, these vibrations will mix. Thus, intense vibrations are present in benzene and all benzene derivatives at $990\text{--}1010\text{ cm}^{-1}$ (DOLLISH *et al.*, 1974), and are therefore diagnostic of the presence of this molecule or its derivatives. A second, weaker ring vibration is observed at 610 cm^{-1} . In benzene derivatives, there are no methylene (H—C—H) vibrations but only bands due to C—H stretches. This leads to the single sharp peak at 3064 cm^{-1} , due to the C—H symmetric stretch. Note that the alkane C—H stretching vibrations

occurred as a broad manifold in the region $2850\text{--}2975\text{ cm}^{-1}$ (Fig. 2a); the intense single peak at 3064 cm^{-1} is therefore distinct from the alkane peaks, and is, with the $990\text{--}1010\text{ cm}^{-1}$ peak, diagnostic of aromatic compounds (GUILHAUMOU, 1982).

Crude oils

Two oil samples from the Hoh accretionary complex were examined to determine both the feasibility of conducting visible Raman spectroscopy on fluorescent, complex hydrocarbon mixtures, as well as to provide a basis for comparison between modern crude oils and the mid-Miocene fluid inclusion described in the following section. The two oil samples were produced by the Jefferson and Medina wells. The Jefferson oil is from the Jefferson Oil Company Hoh Head No. 2 well, located just north of the mouth of the Hoh River in the Olympic National Park. This well was spudded at $\sim 350\text{ m}$ depth in sheared rocks of the Hoh mélange, and produced significant oil production in the 1930's, but was not economic. The other oil in this study comes from the Sunshine Mining Company Medina No. 1 well, located 80 km south of the Jefferson well in the Ocean City area north of Greys Harbor (for the exact location of both wells, see Fig. 1 of KVENVOLDEN *et al.* (1989)). This well was drilled in 1957 and produced 12,000 barrels of 38° gravity oil from sheared Hoh mélange rocks at the 1200 m depth level. Crude oil analyses yielded 35.6% gasoline by volume, 20.5% kerosene, and 42.9% reduced crude. Sulfur contents of the samples were between 0.014 and 0.15 wt.% (KVENVOLDEN *et al.*, 1989). Previous gas chromatographic studies by KVENVOLDEN *et al.* (1989) indicated that the Jefferson and Medina oils had similar molecular weight distributions, which were interpreted to indicate similar source regions and migration histories for these two widely separated samples.

Because of the complexity of the spectra of these hydrocarbons, we will focus principally on the dominant features in each spectrum. Given the wide range of possible vibrations, we view the strongest peaks as being indicative of the dominant chemical species within each sample, while the remainder are likely to be produced by less abundant functional groups. For reference, spectra of mixtures of as few as five to ten hydrocarbon species would be expected to show dozens of peaks in all of the frequency ranges examined here (DOLLISH *et al.*, 1974); this degree of complexity is, not surprisingly, what we observe.

Raman spectra from the Jefferson and Medina oils are similar, but not identical (Fig. 3): this is consistent with gas chromatographic studies (KVENVOLDEN *et al.*, 1989). The spectra from the natural oils include a number of the peaks identified in the synthetic inclusions as discussed in the previous section, and include both chain and cyclic alkanes, unsaturated carbon, and aromatic rings, as well as sulfur complexes. We focus initially on the lowest frequency region of these spectra.

Both oils show a number of peaks in the region between 670 and 950 cm^{-1} (Figs. 3a and 3b). Peaks in this region are probably correlated with either chain or cyclic aliphatic hydrocarbons (DOLLISH *et al.*, 1974). C—C skeletal stretching vibrations are a function of chain length and occur over the range between 850–900 cm^{-1} ; in spectra of both oils, a complex manifold is observed in this region. Cycloalkanes exhibit a distinctive vibration due to ring "breathing" that varies as a function of ring size, from 703 (cyclooctane) to 1188 cm^{-1} (cyclopropane). The cyclohexane ring (a common constituent of hydrocarbons) has a ring breathing vibration that occurs at 802 cm^{-1} . Notably, the frequencies of both alkane and cycloalkane vibrations in this region are somewhat altered by any substitutions for hydrogen. Vibrations in this region could also be produced by internal carbon atoms, such as tert-butyl, isopropyl or quaternary geometries (DOLLISH *et al.*, 1974).

The Jefferson oil also has a number of peaks at 960–1020 cm^{-1} and at 1071 cm^{-1} (Fig. 3a, 3c), whereas the Medina exhibits a smaller manifold centered at 1023 cm^{-1} and a distinctive band at ~ 1077 cm^{-1} (Figs. 3b, 3d). The peaks near 1000 cm^{-1} are in a region which cannot be attributed to vibrations of cycloalkanes or internal carbons, although some substituted C—C stretching vibrations can occur in this region. Benzene, the prototypical aromatic hydrocarbon, has an extremely intense vibration due to the A_{1g} -symmetry ring breathing mode at 990–1010 cm^{-1} , which shifts on substitution of hydrogen by halogens in benzenes to 1060–1100 cm^{-1} for heavy substituents (>25 amu) and 830–620 cm^{-1} for lighter substituents (DOLLISH *et al.*, 1974). Accordingly, the bands near 1000 cm^{-1} are probably produced by aromatic hydrocarbons.

Both the Jefferson and Medina oils have complex manifolds in the 1250 and 1300 cm^{-1} region (Figs. 3c, 3d), while a weak manifold in the Medina that occurs at 1135 cm^{-1} may have a poorly resolved counterpart in the Jefferson oil. The former set of these bands are produced by CH_2 rocking

motions (1175–1310 cm^{-1}), and are thus diagnostic of the presence of CH_2 units (CH_2 twisting vibrations also occur in the range between 720–1060 cm^{-1}). Other carbon configurations also lead to weak peaks in this region of the spectra.

The stretching vibrations of multiply bonded carbons occur in the 1400–2100 cm^{-1} region of the spectra, as well as the CH_2 scissors vibration at 1430–1470 cm^{-1} (Figs. 3e, 3f). The CH_2 is seen in both spectra as a distinctive manifold (due to both symmetric and antisymmetric scissoring motions). For alkanes, these vibrations occur at 1446 to 1473 cm^{-1} , and vary in frequency primarily as a function of the length of the carbon chain and the type of substitutions for hydrogen (DOLLISH *et al.*, 1974), while in alkenes they range from 1389 to 1426 cm^{-1} . Thus, the breadth of this manifold plausibly reflects a range of CH_2 environments being present within these oils.

The peak present near 1500 cm^{-1} is more difficult to uniquely assign, as it could be due to either carbon-nitrogen linkages, C=C stretching within cyclopentadienes, or to vibrations of doubly-bonded carbon-oxygen (although the latter two species are unexpected in natural oils [HUNT, 1979]). In contrast to the 1500 cm^{-1} peak, the strong vibrations at 1604 cm^{-1} (Medina) and 1614 cm^{-1} (Jefferson) are almost certainly produced by the relatively strong ring stretching vibrations of aromatic hydrocarbons. These characteristically occur within 30 cm^{-1} of 1600 cm^{-1} (DOLLISH *et al.*, 1974); thus, this assignment is consistent with our observation of the ring breathing vibration of such species at frequencies near 1000 cm^{-1} . The manifold peak at 1849 cm^{-1} in the Jefferson oil may be due to an additional C=O vibration. We have no simple explanation for the weak band near 2000 cm^{-1} , but believe that it could be associated with any number of triple bonded organic species, consecutive double bonds or possibly an overtone vibration.

In the highest frequency region, both oils show three large peaks at ~ 2420 , 2465, and 2570 cm^{-1} (Figs. 3g, 3h). These are in addition to features at 2848 and 2929 cm^{-1} , which are the expected peaks produced by symmetric and antisymmetric C—H stretching vibrations. The only common functional group giving rise to vibrational bands in the 2400–2600 cm^{-1} region is the thiol (SH) group. Analyses of the Medina oil indicated the presence of sulfur in small concentrations, so some vibrations due to these species are expected, yet these peaks are comparably intense to the C—H stretching vibrations. A possible means through which this en-

Jefferson Oil

Medina Oil

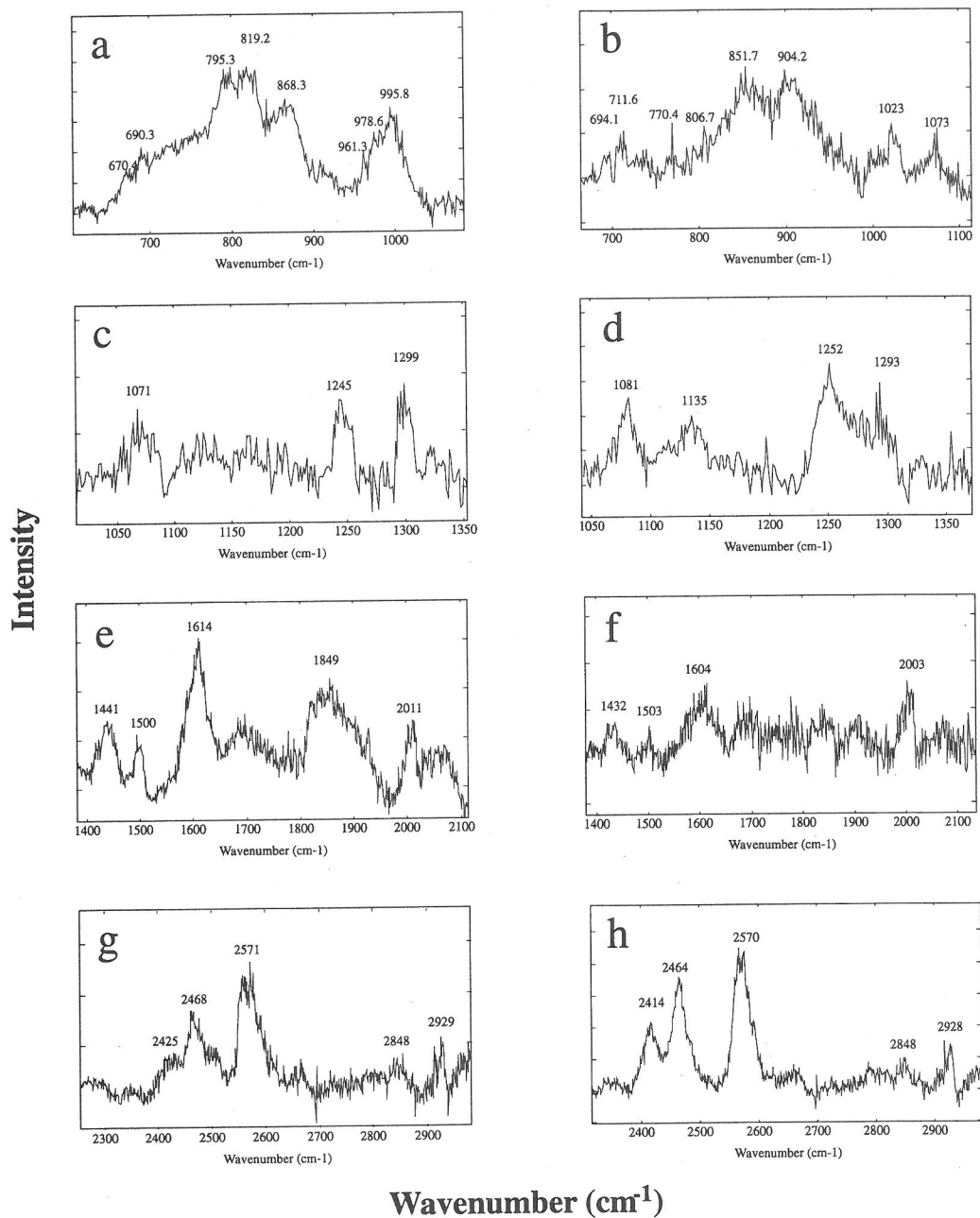


FIG. 3. Raman spectra of complex fluorescent crude oils from the western Olympic Peninsula, Washington. The spectra are notably similar, supporting the gas chromatograph studies of KVENVOL-DEN *et al.* (1989) that indicated similar source regions and migration pathways for these oils, despite the fact that the wells are 80 km apart. Peaks are related to the species that are present, and include alkanes, cycloalkanes, aromatic hydrocarbons (benzene) and sulfur. See text for discussion.

hancement in intensity could be generated is through a resonance Raman effect (e.g., MELVEGER, 1978). Such resonance effects have been extensively documented to occur in sulfonated species, although typically under blue-green laser excitation: this resonance is induced by an electronic transition associated with sulfur within hydrocarbons (e.g., DELLA VEDOVA, 1992). Because of the weakness of our non-resonant hydrocarbon spectra, it is possible that even a weak resonance enhancement of the Raman intensity of these bands could produce a significant augmentation of their intensity beyond that expected from the abundance of sulfonated species in the sample. In natural oils, sulfur can occur either as H_2S or as a substituent in higher order hydrocarbons (HUNT, 1979). If sulfur is present as part of a hydrocarbon, then the $S=C$ stretching vibration might be expected to be observed in the $800\text{--}1065\text{ cm}^{-1}$ region, with the $S-C$ stretch in the $620\text{--}715\text{ cm}^{-1}$ region. Both vibrations occur in the same region as the $C-C$ stretch and cycloalkane ring breathing frequencies. Thus, we cannot preclude that some of the peaks in this region may be produced by organosulfur species.

Natural fluid inclusions

The particular sample analyzed here comes from a 40 m thick fault zone related to the main phase of compressional deformation in the Hoh accretionary complex. The family of inclusions analyzed occur as $\sim 20\text{ }\mu\text{m}$ diameter secondary inclusions in a late syn-deformational sparitic calcite vein.

In the low frequency region (below 1100 cm^{-1}), our Raman spectra contain peaks from both the host calcite mineral and the hydrocarbon inclusions (Fig. 4; for peak assignments see Table 1). Vibrations assignable to the calcite include the CO_3 symmetric stretching vibration at 1087 cm^{-1} , as well as the CO_3 symmetric bending vibration at 722 cm^{-1} (WHITE, 1974). In addition to the carbonate peaks, this spectral region is characterized by a multitude of peaks and manifolds in the 700 to 950 cm^{-1} region, which are produced by the hydrocarbons and are similar to the peaks seen in the oil samples. Most, if not all, of these peaks can be assigned to the $C-C$ stretching vibration of alkanes, the breathing vibrations of cycloalkanes, or vibrations related to internal carbon configurations (Table 1). The 990 to 1010 cm^{-1} region, however, is of particular interest. As observed in the bromobenzene synthetic inclusion and both oil samples, peaks in this spectral region are diagnostic of the

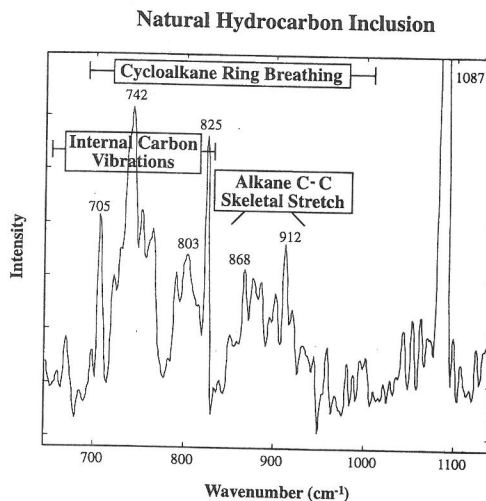


FIG. 4. Raman spectrum of a natural hydrocarbon inclusion from the Hoh accretionary complex, Olympic Peninsula, Washington. Peak assignments are listed in Table 1. Note the symmetric stretching peak of the carbonate unit at 1087 cm^{-1} , and the manifolds at 700 to 750 cm^{-1} , 803 cm^{-1} , and $850\text{--}920\text{ cm}^{-1}$. These vibrations can be assigned to alkanes or cycloalkanes, with a component produced by the symmetric bending vibration of the carbonate group present near 720 cm^{-1} . No major peaks are visible near 1000 cm^{-1} , where a strong vibration of benzene and its derivatives occurs.

presence of aromatic rings. These vibrations (because of their highly symmetric character) are quite intense, and we would expect to observe them if benzene (or its derivatives) were present in abundance in the sample. Because such peaks are absent in this inclusion, benzene or substituted benzenes (if present) must be in concentrations significantly lower than within the oil samples.

In the mid-frequency range, there are two manifolds observed near 1440 cm^{-1} and 1650 cm^{-1} (Fig. 5; see peak assignments listed in Table 2). Although one of the peaks in the 1440 cm^{-1} manifold could be due to the antisymmetric stretching vibration of the carbonate group (WHITE, 1974) or the symmetric stretch of the carboxylate ion group (LIN-VIEN *et al.*, 1991). The other peaks in this region are plausibly assigned to the methylene (CH_2) scissors vibrations seen in the synthetic alkanes, cycloalkanes and oils (Table 2). The other high intensity region in this spectrum is centered at 1650 cm^{-1} , which could be associated with the presence of carbonyl groups; such groups are relatively common constituents of crude oils (HUNT, 1979). We note that because

Table 1. Natural hydrocarbon inclusion, 650-1150 cm^{-1} .

n-alkane vibrations:	C-C stretch (DOLLISH <i>et al.</i>)	identified peak
n-butane	837	--
n-pentane	869	868
n-hexane	898	900
n-heptane	905	in manifold?
n-octane	899	900
n-nonane	888	886
n-decane	886	886
n-dodecane	892	894
n-hexadecane	888	886

Strong peaks in the 800-1000 cm^{-1} range are very common for all alkanes, and (although not diagnostic) are due to various combinations of C-C stretching and CH_3 (methyl) twisting-rocking (DOLLISH *et al.*, 1974).

Additional strong peaks due to the configuration of carbon atoms:

tert-butyl	680-750
isopropyl	740-830
internal quaternary carbon atom	670-710
internal tertiary carbon atom	800-860
two adjacent tertiary carbon atoms	730-760

(Note: these latter peaks are not diagnostic, as they vary as a function of the base chain of which they are a part.)

cycloalkane vibrations	ring breathing (DOLLISH <i>et al.</i>)	identified peak
cyclobutane	1001	1002
cyclopentane	886	886
cyclohexane	802	803
cycloheptane	733	735 (shoulder on low frequency side of 742 peak?)
cyclooctane	703	705
benzene and its derivatives	990-1010	--

there is no prominent peak in the 1000 cm^{-1} region (diagnostic of aromatic hydrocarbons), we cannot attribute the 1600 cm^{-1} peak to the weaker band expected in substituted benzene rings. A single band is also present near 1540 cm^{-1} in the spectrum of the natural fluid inclusion (Fig. 5). We have no simple assignment for the origin of this feature, but note that peaks in this region of the spectrum could be generated by vibrations associated with carbon-nitrogen linkages (we do not view the assignment of this band to $\text{C}=\text{C}$ species as likely, due to the scarcity of such species in natural oils [HUNT, 1979]). Alternatively, this peak could be generated by either a combination band or a resonance enhanced vibration (or overtone) of a sulfonated species.

Vibrations related to C—H stretching occur as a manifold centered at 2919 cm^{-1} , with numerous other weaker peaks occurring throughout the frequency range between 2825 and 3095 cm^{-1} (Fig. 6). This manifold is due to the juxtaposition of

symmetric and antisymmetric vibrations of hydrocarbon compounds containing single bonded carbons. For example, the peak at 2911 cm^{-1} may plausibly be associated with either methane or the methylene antisymmetric stretch, the 2924 cm^{-1} band with ethane or the methyl antisymmetric stretch, and the 2945 cm^{-1} due to the methyl and methylene antisymmetric and symmetric stretches (GUILHAUMOU, pers. comm.). Almost all of these peaks can in fact be assigned to alkanes or cycloalkanes (Table 3). Higher frequency C—H vibrations (3000 to 3100 cm^{-1}) can be assigned to C—H stretching from either alkenes or aromatic compounds. The lack of a significant peak at 3062 cm^{-1} argues against there being a significant amount of benzene in this sample, consistent with the lack of a ring breathing peak observed in the lower frequency spectral region.

Thus, for this natural fluid inclusion from the Hoh accretionary complex, we find compelling evidence

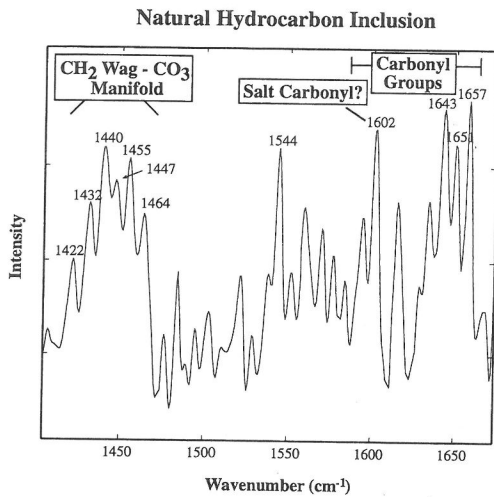


FIG. 5. Raman spectrum of a natural hydrocarbon inclusion from the Hoh accretionary complex, Olympic Peninsula, Washington. Peak assignments are listed in Table 2. The two manifolds seen in this spectra are due to the H-C-H methylene scissors vibrations (1420 to 1465 cm^{-1}) and carboxylic acid. The vibration near 1540 cm^{-1} may be associated with carbon-nitrogen bonds; see text for discussion.

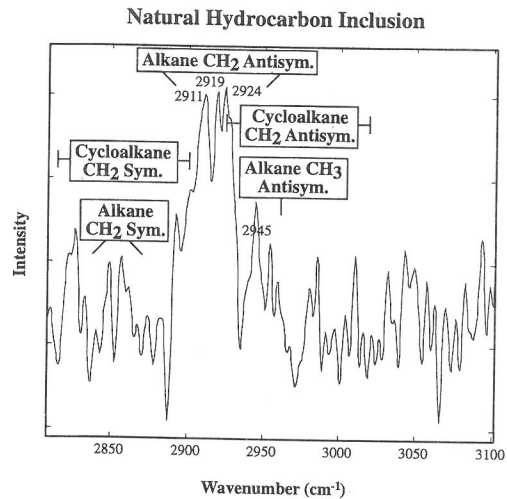


FIG. 6. Raman spectrum of a natural hydrocarbon inclusion from the Hoh accretionary complex, Olympic Peninsula, Washington. Peak assignments are listed in Table 3. The large manifold peak near 2900 cm^{-1} is indicative of alkane and cycloalkane methyl and methylene symmetric and antisymmetric stretching vibrations. Note the lack of a significant peak at 3062 cm^{-1} , indicating the absence of appreciable quantities of benzene or its derivatives.

for the presence of alkanes and cycloalkanes. Evidence for the presence of aromatic hydrocarbons (benzene and its derivatives) within these inclusions is notably lacking. For comparison, the Raman spectra of the oils document the presence of alkanes, cycloalkanes and aromatic rings, as well as indications of the presence of sulfur.

Comparison between oils and inclusion with possible causes of chemical differences

Whereas spectra from the oil samples are similar to the natural hydrocarbon inclusion, there is one highly significant difference. Like the oil samples, the inclusion contains alkanes and cycloalkanes.

Table 2. Natural hydrocarbon inclusion, 1400 - 1675 cm^{-1} .

compound	methylene scissors (DOLLISH <i>et al.</i>)	identified peak
alkane, in-plane	1446-1473	large manifold peak, 1447-1464
alkane, out-of-plane	1465	1464
cyclobutane	1443	1440
cyclopentane	1455	1455
cyclohexane	1452	1455
cycloheptane	1450	1447
cyclooctane	1467	1464
alkenes, and substituted alkenes (?)	1389-1426	1422, 1432
compound	expected peak	identified peak
carboxylic acid*	~ 1650	manifold at 1643-1657
alkenes, and substituted alkenes (??)	1575-1693	1602, 1616, etc.
cycloalkenes (??)	1614-1672	1626-1657

*Note: alkenes and substituted alkenes have C=C vibrations in this region, yet these unsaturated hydrocarbon constituents are extremely rare in naturally occurring oils [HUNT, 1979]; we thus attribute vibrations in this region to carboxylic acid.

Table 3. Natural hydrocarbon inclusion, 2800-3100 cm^{-1} . This zone is entirely due to the various C-H stretching modes, and is indicative of the compounds present.

compound	CH ₃ antisym. stretch (DOLLISH <i>et al.</i>)	identified peak	CH ₃ sym. stretch (DOLLISH <i>et al.</i>)	identified peak
alkanes and derivatives	2965-2969	2959 and shoulder?	2884	2892?
compound	CH ₂ antisym. stretch (DOLLISH <i>et al.</i>)	identified peak	CH ₂ sym. stretch (DOLLISH <i>et al.</i>)	identified peak
cyclopropane	3101-3090	3093	3038-3019	3032
cyclobutane	2987-2975	2985	2895-2887	2892
cyclopentane	2959-2952	2959, 2954	2866-2853	2861, 2857
cyclohexane	2933-2915	in 2924 manifold	2897-2852	numerous peaks
cycloheptane	2935-2917	in 2924 manifold	2862-2851	2861, 2857
cyclooctane	2925	2924	2855	2857
alkanes	2929-2912	in 2919 manifold	2861-2849	2861, 2857, 2849

The Raman spectrum of the inclusion, however, contains little, if any, evidence for the existence of benzene or substituted benzenes. We suggest that the different histories of the oil and the inclusion led to their spectroscopic differences. Both the oil and the inclusion come from sheared rocks within the Hoh rock assemblage. The oils were recently extracted from pore spaces in near-surface rocks, while the inclusion is fundamentally different. Since the inclusion is part of a vein, the hydrocarbons (unless they are locally derived) must have traveled in the dominantly aqueous system that deposited the carbonate vein. The vein the inclusion occurs in was emplaced during thrusting in Miocene time (ORANGE *et al.*, 1991, 1993) at conditions in the range of 50–100 MPa and 80–100°C (ORANGE *et al.*, 1992).

Differences between the oils and the hydrocarbon inclusion could be due to differences in age, source region, migration, and alteration (TISSOT and WELTE, 1984). Since both the oils and the inclusion occur in sheared Miocene Hoh rocks related to large scale thrusting on the Olympic Peninsula we believe that they are likely to have similar ages, migration histories, and source regions. Gas chromatograph studies of petroliferous samples throughout the Hoh accretionary complex support this hypothesis (KVENVOLDEN *et al.*, 1989). Thus, the chemical differences between the oil and the inclusion may be due to the alteration history. The oil within the inclusion may have experienced higher temperatures than the oils, leading to thermal degradation. Benzene is stable at relatively

high temperatures, and so the lack of benzene can not be attributed to high temperature alteration. Benzene is, however, quite soluble in aqueous solutions. The high surface area to volume ratio in the fluid inclusion could have led to preferential removal of benzene by water washing, which selectively removes lighter hydrocarbon molecules from their source as these compounds are much more soluble in aqueous solution (TISSOT and WELTE, 1984; WELTE *et al.*, 1982; LAFARGUE and BARKER, 1988).

CONCLUSIONS

Visible Raman spectroscopy can successfully identify the major vibrational modes within synthetic hydrocarbon inclusions, complex fluorescent oils, and fluorescent natural hydrocarbon inclusions in calcite. The synthetic inclusions analyzed represent alkanes, cycloalkanes, and benzene derivatives. Problems related to fluorescence and photodegradation in natural inclusions and their matrix can be avoided by using judiciously selected, longer laser excitation wavelengths, low laser power and long integration times. Oil samples provide similar problems with fluorescence that can be overcome again by selecting longer laser wavelengths and increasing the detector integration times.

This technique is capable of determining what type of hydrocarbon species are present in abundance within such inclusions, based on the presence or absence of characteristic vibrational bands

of organic functional groups. We note that at present, because of the complications associated with quantification of the relative Raman scattering cross-sections of the range of different hydrocarbons likely to be present in such fluid inclusions, this technique remains a qualitative tool capable of characterizing which types of organic functional groups are present in abundance within inclusions (e.g., WOPENKA and PASTERIS, 1986).

Determining the geochemical history of hydrocarbon evolution in a complex geologic region such as the Hoh accretionary complex clearly requires more detailed data on the temporal evolution of inclusion chemistry. However, we have used variations in Raman spectra to derive some qualitative (and geologically consistent) insights into possible differences in migration histories between a mid-Miocene inclusion and present-day crude oils from the same complex. Although the regional applicability of these results remains uncertain, they demonstrate the utility of Raman spectroscopy as a powerful tool for fingerprinting hydrocarbons and for identifying the major functional groups within each sample.

Acknowledgments—We would like to thank J. Pironon for his generous contribution of the synthetic hydrocarbon inclusion samples. Keith Kvenvolden provided valuable insight into the organic geochemistry of hydrocarbon species. We thank J. J. Freeman, R. J. Hemley, K. Kvenvolden, J. C. Moore, and J. Gieskes for helpful reviews which improved this paper. This research was partially supported by the W. M. Keck Foundation, Weyerhaeuser Corporation, the National Science Foundation and the American Chemical Society-Petroleum Research Fund. E. K. is an A. P. Sloan Foundation Fellow. Institute of Tectonics (Mineral Physics Lab) Contribution No. 111.

REFERENCES

- BARRES O., BURNEAU A., DUBESSY J. and PAGEL M. (1987) Application of micro-FT-IR spectroscopy to individual hydrocarbon fluid inclusion analysis. *Appl. Spectr.* **41**, 1000–1008.
- BECKER R. S. (1969) *Theory and interpretation of fluorescence and phosphorescence*. Wiley-Interscience.
- BERLMAN B. (1965) *Handbook of Fluorescence Spectra of Aromatic Molecules*. Academic Press, New York.
- BURDETT R. A. and TAYLOR L. W. (1955) Determination of aromatic hydrocarbons in lubricating oil fractions by far ultra-violet absorption spectroscopy. In *Molecular Spectroscopy, report of a conference organized by The Spectroscopic Panel of the Hydrocarbon Research Group of the Institute of Petroleum, London, 28–29 October 1954* (ed. G. SELL), 30–41.
- BURRUSS R. C. (1981) Hydrocarbon fluid inclusions in studies of sedimentary diagenesis. In *Mineralogical Association of Canada Short Course on Fluid Inclusions: Applications to Petrology* (eds. L.S. HOLLISTER and M.L. CRAWFORD), vol. 6, pp. 138–156. Mineralogical Association of Canada.
- BURRUSS R. C., CERCONE K. R. and HARRIS P. M. (1983) Fluid inclusion petrography and tectonic-burial history of the Al Ali No. 2 well: Evidence for the timing of diagenesis and oil migration, northern Oman Foredeep. *Geology* **11**, 567–570.
- BURRUSS R. C., CERCONE K. R. and HARRIS P. M. (1985) Timing of hydrocarbon migration: evidence from fluid inclusions in calcite cements, tectonics, and burial history: in *Carbonate Cements* (eds. N. SCHNEIDERMANN and P. M. HARRIS), Special Publication No. 36, pp. 277–289. Society of Economic Paleontologists and Mineralogists.
- BURRUSS R. C., GING T. and CARLSON, D. (1989) Raman microprobe observations of carbon and oxygen stable isotopes in geologic materials. In *Microbeam Analysis - 1989* (ed. P. E. RUSSELL), pp. 173–175. San Francisco Press.
- CHOU I.-M., PASTERIS J. D. and SEITZ J. C. (1990) High-density volatiles in the system C-O-H-N for the calibration of a laser Raman microprobe. *Geochim. Cosmochim. Acta* **54**, 535–543.
- COWAN D. O. and DRISKO R.L. (1976) *Elements of Organic Photochemistry*. Plenum.
- DAWSON W. R. and WINDSOR M. W. (1968) Fluorescence yields of aromatic compounds. *J. Phys. Chem.* **72**, 3251.
- DELE-DUBOIS M.-L., DHAMELINCOURT P. and SCHNUBEL H.-J. (1980) Studies by Raman spectroscopy of inclusions in diamonds, sapphires, and emeralds, parts 1 and 2. *Rev. Gemmologie*, **63**, 11–14 (part 1), and **64**, 13–16 (part 2) (in French).
- DELLA VEDOVA C. O. (1992) Towards the absolute determination of the conformation in thioester compounds through the first pre-resonance Raman study in X-NSO molecules, *J. Molec. Struct.* **274**, 9–23.
- DIAS J. R. (1987) *Handbook of Polycyclic Hydrocarbons: Part A Benzenoid Hydrocarbons*. Elsevier, Amsterdam.
- DOLLISH F. R., FATELEY W. G. and BENTLEY F. F. (1974) *Characteristic Raman frequencies of organic compounds*, John Wiley and Sons, New York.
- ENGLMAN, R. (1979) *Non-radiative decay of ions and molecules in solids*, 336 pp., North-Holland Publishing Co., New York.
- ETMINAN H. and HOFFMAN C.F. (1989) Biomarkers in fluid inclusions: A new tool in constraining source regimes and its implications for the genesis of Mississippi Valley-type deposits. *Geology* **17**, 19–22.
- FRANTZ J. D., VIRGO D. and MYSEN B. O. (1982) Time-lapse spectroscopy for fluorescence radiation rejection, *Carnegie Institute of Washington Year Book 81*, 437–440.
- GAUTIER D. L., KHARAKA Y. K. and SURDAM R. C. (1985) Relationship of Organic Matter and Mineral Diagenesis, SEPM Short Course No. 17, Tulsa, OK.
- GUILHAUMOU N. (1982) Accurate analysis of fluid inclusions by the laser molecular microprobe (MOLE) and by microthermometry. *Travaux Lab. Géol. Ecole Normale Supérieure*, **14**, 68 p. (in French).
- GUILHAUMOU N. and SZYDLOWSKI N. (1989) Analyse ponctuelle à micro FTIR des inclusions d'hydrocarbures de H.Zriba-Guebli. Mise en évidence de modifications par surchauffe sous pression de confinement (300 C - 40 Mpa). *C. R. Acad. Sci. Paris* **309**, series II, 1171–1176.

- GUILHAUMOU N., JOUAFFRE D., VELDE B. and BÉNY C. (1988) Raman microprobe analysis on gaseous inclusions from diagenetically altered Terres Noures (S-E, France). *Bull. Mineral.* **111**, 577–585.
- HUNT J. M. (1979), *Petroleum Geochemistry and Geology*, 617 pp., W.H. Freeman, San Francisco.
- HASZELDINE R. S., SAMSON I. M. and COMFORD C. (1984) Dating diagenesis in a petroleum basin, a new fluid inclusion method. *Nature* **307**, 354–357.
- HORSFIELD B. and MCLIMANS R. K. (1984) Geothermometry and geochemistry of aqueous and oil-bearing fluid inclusions from Fateh Field, Dubai. *Org. Geochem.* **6**, 733–740.
- JENSENIUS J. and BURRUSS R. C. (1990) Hydrocarbon-water interactions during brine migration: Evidence from hydrocarbon inclusions in calcite cements from Danish North Sea oil fields. *Geochim. Cosmochim. Acta* **54**, 705–713.
- KVENVOLDEN K. A. and ROEDDER E. (1971) Fluid inclusions in quartz crystals from South-West Africa. *Geochim. Cosmochim. Acta* **35**, 1209–1229.
- KVENVOLDEN K. A., RAPP J. B., HOSTETTLER F. D. and SNAVELY P. D. Jr. (1989) Preliminary Evaluation of the Petroleum Potential of the Tertiary Accretionary Terrane, West Side of the Olympic Peninsula, Washington: Part 2 - Comparison of Molecular Markers in Oil and Rock Extracts. *U.S. Geol. Survey Bull.* **1892**, p. 19–36.
- LAFARGUE E. and BARKER C. (1988) Effect of water washing on crude oil composition. *Bull. Amer. Assoc. Petrol. Geol.* **72**, 263–276.
- LIN-VEIN D., COLTHUP N.B., FATELEY W.G. and GRASSELLI J.G. (1991) *The Handbook of Infrared and Raman Characteristic Frequencies of Organic Molecules*, Academic Press, New York.
- MCLIMANS R. K. (1987) The application of fluid inclusions to migration of oil and diagenesis in petroleum reservoirs. *Appl. Geochem.* **2**, 585–603.
- MCLIMANS R. K. and VIDETICH P.E. (1987) Reservoir diagenesis and oil migration, Middle Jurassic Great Oolite Limestone, Weldon Basin, Southern England. In *Petroleum Geology of North West Europe* (ed. J. BROOKS and K. GLENNIE), pp. 419–429. Graham and Trodman.
- MEDLIN W. L. (1968) The nature of traps and emission centers in thermoluminescent rock materials. In *Thermoluminescence of Geologic Materials* (ed. D. J. McDUGALL), pp. 193–223. Academic Press, New York.
- MELVEGER, A.J. (1978) *Resonance Raman Spectroscopy as an Analytic Tool*, Franklin Inst. Press, Philadelphia.
- MURRAY R. C. (1957) Hydrocarbon fluid inclusions in quartz. *Bull. Amer. Assoc. Petrol. Geol.* **41**, 950–956.
- NAKAMOTO K. (1982) *Infrared and Raman Spectra of Inorganic and Coordination Compounds*. 4th Ed., Wiley-Interscience, New York.
- NOONER D. W., UPDEGROVE D. A., FLORY D. A., ORO J. and MUELLER G. (1973) Isotopic and chemical data of bitumens associated with hydrothermal veins from Windy Knoll, Derbyshire, England. *Chem. Geol.* **11**, 189–202.
- O'GRADY M. R., BODNAR R. J., HELLGETH J. W., CONROY C. M., TAYLOR L. T. and KNIGHT C. L. (1989) Fourier transform infrared microprobe (FTIRM) analysis of individual petroleum fluid inclusions in geologic samples. In *Microbeam Analysis* (ed. P. E. RUSSELL), pp. 579–582. San Francisco Press.
- ORANGE D. L., GEDDES D., COX R. and UNDERWOOD M. (1991) Out-of-Sequence Thrust Faulting in a Young Accretionary Complex: Evidence from Fluid Inclusion and Vitrinite Reflectance Data. *EOS (Trans., Amer. Geophys. Union)*, **44**, 549.
- ORANGE D. L., GEDDES D., MOORE J. C., COX R. and UNDERWOOD M. (1992) Constraining the temperature, pressure, and fluid compositional evolution of an accretionary complex by an integrated study of cement stratigraphy and tectonics, *7th International Conference on Water-Rock Interaction, Park City, Utah*, (eds. Y. KHARAKA and A. MAEST), Balkema, Rotterdam, p. 1537–1541.
- ORANGE D. L., GEDDES D., and MOORE J. C. (1993) Structural and fluid evolution of a young accretionary complex: The Hoh rock assemblage of the western Olympic Peninsula, Washington. *Geol. Soc. of Amer. Bull.* **105**, 1053–1075.
- PAGEL M., WALGENWITZ F. and DUBESSY J. (1986) Fluid inclusions in oil and gas-bearing sedimentary formations. In *Thermal Modeling in Sedimentary Basins*, pp. 565–583. Ed. Technip., Paris.
- PASTERIS J. D., PATEL R., BERGMAN S. C. and ADAR F. (1983) Comparative spectroscopy and microthermometry on fluid inclusions in a mantle xenolith. *EOS (Trans., Amer. Geophys. Union)*, **64**, 340.
- PASTERIS J. D., SEITZ J. C. and WOPENKA B. (1985) Compositional interpretation of synthetic C—O—H fluid inclusions by micro-Raman analysis and microthermometry. In *Microbeam Analysis—1985* (ed. J. T. ARMSTRONG), pp. 25–28. San Francisco Press.
- PASTERIS J. D., WOPENKA B. and SEITZ J. C. (1988) Practical aspects of quantitative laser Raman microprobe spectroscopy for the study of fluid inclusions. *Geochim. Cosmochim. Acta* **52**, 979–988.
- PERING K.L. (1973) Bitumens associated with lead, zinc and fluorite ore minerals in North Derbyshire, England. *Geochim. Cosmochim. Acta* **37**, 401–417.
- PIRONON J. (1990) Synthesis of hydrocarbon fluid inclusions at low temperature. *Amer. Mineral.* **75**, 226–229.
- PIRONON J. and BARRES O. (1990) Semi-quantitative FT-IR micronanalysis limits: Evidence from synthetic hydrocarbon fluid inclusions in sylvite. *Geochim. Cosmochim. Acta* **54**, 509–518.
- PIRONON J., SAWATZKI J. and DUBESSY J. (1991) NIR FT-Raman microspectroscopy of fluid inclusions - Comparisons with Vis Raman and FT-IR microspectroscopies. *Geochim. Cosmochim. Acta* **55**, 3885–3891.
- RAU W. W. (1973) Geology of the Washington Coast between Point Grenville and the Hoh River. *Washington Department of Natural Resources, Geology and Earth Resources Division, Bulletin* no. 66, 58 p.
- RAU W. W. (1975) Geologic map of the Destruction Island and Taholah Quadrangles, Washington. *State of Washington Department of Natural Resources, Division of Geology and Earth Resources*, scale 1:62,500, Geologic Map GM-13.
- RAU W. W. (1979) Geologic map in the vicinity of the Lower Bogachiel and Hoh rivers, and the Washington Coast. *Washington Department of Natural Resources, Division of Geology and Earth Resources, Geologic Map GM-24*.
- ROEDDER E. (1984) *Fluid Inclusions. Reviews in Mineral-*

- ogy, 12, Mineralogical Society of America, Washington, D.C.
- ROSASCO G. J. and ROEDDER E. (1979) Application of a new Raman microprobe spectrometer to nondestructive analysis of sulfate and other ions in individual phases in fluid inclusions in minerals. *Geochim. Cosmochim. Acta* **43**, 1907–1915.
- Sadtler Handbook of UV Spectra* (1982) (ed W. W. Simmons) Sadtler Research Laboratories, Philadelphia, PA.
- SEITZ J. C., PASTERIS J. D. and WOPENKA B. (1987) Characterization of CO₂-CH₄-H₂O fluid inclusions by microthermometry and laser Raman microprobe spectroscopy: Inferences for clathrate and fluid equilibria. *Geochim. Cosmochim. Acta* **51**, 1651–1664.
- SEITZ J. C., PASTERIS J. D. and CHOU I.-M. (1989) Quantitative composition and density determinations of CH₄-N₂-bearing fluid inclusions by Raman micro-spectroscopy. *Geol. Soc. Amer. Abstr. Prog.* **21**, A358.
- TEN HAVE T. and HEIJNEN W. (1985) Cathodoluminescence activation and zonation in carbonate rocks: an experimental approach. *Geol. Mijnbouw* **64**, 297–310.
- TISSOT B. P. and WELTE D. H. (1984) *Petroleum Formation and Occurrence*, Springer-Verlag, New York.
- TOURAY J. C., BENY-BASSEZ C., DUBESSY J. and GUILHAUMOU N. (1985) Microcharacterization of fluid inclusions in minerals by Raman microprobe. *Scanning Electron Microscopy, Vol. 1, SEM Inc.*, pp. 103–118. AMF O'Hare.
- VEIRS D.K., CHIA V.K.F. and ROSENBLATT G.M. (1987) Raman spectroscopy applications of an imaging P.M.T., *Appl. Optics* **26**, 3530–3535.
- WALKER G., ABUMERE O. E. and KAMALUDDIN B. (1989) Luminescence spectroscopy of Mn²⁺ centres in rock-forming carbonates. *Mineral Mag.* **53**, 201–211.
- WELTE D. H., KRATOCHVIL H., RULLKOTTER J., LADWEIN J. and SCHAEFER R. G. (1982) Organic geochemistry of crude oils from the Vienna basin and an assessment of their origin. *Chem. Geol.* **35**, 33–68.
- WHITE, W.B. (1974) The carbonate minerals. In *The Infra-red Spectra of Minerals* (ed. V.C. FARMER), pp. 227–279. Mineralogical Society, London.
- WOPENKA B. and PASTERIS J.D. (1986) Limitations to quantitative analysis of fluid inclusions in geological samples by laser Raman microprobe spectroscopy. *Appl. Spectroscopy* **40**, 144–151.
- WOPENKA B., PASTERIS J. D. and FREEMAN J. J. (1990) Analysis of individual fluid inclusions by Fourier transform infrared and Raman microspectroscopy. *Geochim. Cosmochim. Acta* **54**, 519–533.

